The effect of oxide additions on medium-range order structures in borosilicate glasses

2007 J. Phys.: Condens. Matter 19 415114

(http://iopscience.iop.org/0953-8984/19/41/415114)

IOP PUBLISHING JOURNAL OF PHYSICS: CONDENSED MATTER

J. Phys.: Condens. Matter **19** (2007) 415114 (12pp) doi:10.1088/0953-8984/19/41/415114

The effect of oxide additions on medium-range order structures in borosilicate glasses

B G Parkinson[1], D Holland[1], M E Smith[1], A P Howes[1] and C R Scales[2]

[1] Department of Physics, Warwick University, Coventry CV4 7AL, UK
[2] Nexia Solutions, Sellafield, Seascale, Cumbria CA20 8PG, UK

E-mail: d.holland@warwick.ac.uk

Received 23 April 2007, in final form 24 April 2007
Published 27 September 2007
Online at stacks.iop.org/JPhysCM/19/415114

Abstract

Boron-11 nuclear magnetic resonance (MAS NMR) and Raman spectroscopies have been used to study four families of glasses: $x\mathrm{Cs_2O}(100-x)\mathrm{ZMW}(0 < x < 10)$, where ZMW represents the borosilicate glass MW to which oxides Z (Al_2O_3, La_2O_3 and MgO) are added such that, overall, $1.0 \leqslant R$ (=[modifier]/[B_2O_3]) $\leqslant 2.5$; K (=[SiO_2]/[B_2O_3]) $= 3.2$. These glasses are related to the system used for the vitrification of high-level nuclear waste. The spectra reveal the presence of reedmergnerite and danburite medium-range order structural units in the glasses. The fraction of danburite units increases with the addition of caesium oxide when Al_2O_3 or La_2O_3 are present, and decreases when MgO is present.

1. Introduction

Zachariasen [1] introduced the notion of the *continuous random network* (CRN) in glasses, which is based on coordination polyhedra that are closely similar to those in the related crystalline forms but which are connected to each other with a distribution of dihedral angles, such that there is no order beyond that associated with the first coordination sphere (short-range order). However, this theory had to be revised with the observation of medium (or intermediate)-range order structures (MRO) within a variety of glasses [2–11].

Borate-containing glasses, such as alkali borate and borosilicate glasses, have long been an area of interest because of the nonlinear change of their properties with composition, due to the change from three-coordinated (B_3) to four-coordinated (B_4) and then to three-coordinated boron $(B_3)^-$ sites as a function of increasing alkali oxide modifier content [12–19]. The presence of MRO borate structural units (often referred to as superstructural units) in these glasses was confirmed relatively recently. Neutron scattering [20–22] and Raman spectroscopy studies [23, 18] showed that a variety of MRO units exist throughout the compositional range of alkali borate glasses, and it is believed that it is these units which are the origin of the multiple four-coordinated boron sites observed using ^{11}B magic angle spinning, nuclear magnetic resonance (MAS NMR) spectra [24, 9].

MRO units have also been found in mixed-oxide borosilicate glasses in the Raman spectroscopy studies carried out by Utegulov *et al* [25] and Bunker *et al* [26], with their presence again being linked with multiple BO_4 sites observed in the ^{11}B MAS NMR work by Du *et al* [27], similar to those observed by Anguiar and Kroeker [24, 9] in alkali borates. These borosilicate mineral superstructures, in the form of reedmergnerite $[BSi_3O_8]^-$ and danburite $[B_2Si_2O_8]^{2-}$ units, have different four-coordinated boron environments; reedmergnerite having one B_4 group per unit with four silicon next-nearest neighbours, and danburite containing two B_4 groups per unit with three silicon next-nearest neighbours and one boron next-nearest neighbour.

Many studies have been made of borosilicate glasses using MAS NMR and Raman spectroscopy [28, 29, 14, 30, 31, 27, 32]. These have focussed on changes in the structure of the borate and silicate glass networks, as a function of alkali content. Structural studies, using ^{11}B, ^{29}Si and ^{17}O (MAS NMR), have led to widely accepted models for both the borate and borosilicate systems [28, 29, 14, 33]. The addition of a glass modifier to a borate glass network initially converts trigonal planar, three-coordinated boron in $[BO_3]$ units (B_3) to tetrahedral, four-coordinated boron in $[BO_4]^-$ units (B_4). At higher modifier concentrations, B_4 are replaced by B_3^-, i.e. trigonal planar $[BO_3]^-$ with one non-bridging oxygen. Trivalent oxides, Z_2O_3, such as Al_2O_3, Fe_2O_3 or La_2O_3 act as intermediate oxides, removing modifying alkali oxide from the borate glass network to charge compensate $[ZO_n]^-$ ions and hence lower the fraction of four-coordinated boron sites (N_4) [34]. The trend in N_4 differs between the borate and borosilicate glass systems, although both are nonlinear in nature, because modifier ions may also associate with various Q^n silicate units (where n is the number of bridging oxygens –Si–O–Si– and $4 - n$ is the number of non-bridging oxygens –Si–O^- which are charge balanced by the modifier cation M^+). The most accurate N_4 model to date for the alkali borosilicate glass system ($RM_2O{\cdot}KSiO_2{\cdot}B_2O_3$) is that of Dell *et al* [14], although recently ^{11}B NMR measurements [30] have shown this model to be incorrect for $R > 0.5$, where R is the ratio of alkali oxide to boron oxide content. According to the Dell model, in the range $0 \leqslant R \leqslant 0.5$, all alkali oxide modifier is used to convert B_3 to B_4. This continues for $0.5 \leqslant R \leqslant 0.5 + K/16$ with the additional stabilization of B_4 units by their combination with Q^4 units to form reedmergnerite-like groups. The B_4 unit has all Q^4 next-nearest neighbours. The formation of new B_4 ceases when all Q^4 become incorporated into the reedmergnerite units at $R = 0.5 + K/16$. For $0.5 + K/16 \leqslant R \leqslant 0.5 + K/4$, all additional alkali oxide is used to convert Q^4 to Q^3, and therefore N_4 remains constant. At $R = 0.5 + K/4$ and beyond, there is the additional process of conversion of B_3 and B_4 to B_3^- and B_3^{2-}, and N_4 decreases linearly to eventually reach zero at $R = 2 + K$.

Raman spectroscopy has been used to detect superstructural units in alkali borate glasses which relate to those seen in the corresponding crystal and mineral units [26, 22, 35, 23]. However, limited work has been carried out on alkali borosilicate glass systems [26, 36].

In this study, four caesium-containing mixed-oxide alkali borosilicate glass systems, containing aluminium oxide, lanthanum oxide or magnesium oxide are investigated using ^{11}B and ^{29}Si MAS NMR and Raman spectroscopy, to obtain information on how these additional three oxides affect the presence of the superstructural units based on reedmergnerite and danburite. These four borosilicate glass systems are part of a larger study into the origin of undesirable volatilization of material from these melts at high temperature.

2. Experimental details

2.1. Sample preparation

Four modified mixed-alkali borosilicate glass systems (CsAlMW, CsLaMW, CsMgMW and CsMg′MW) were made at the compositions $x\mathrm{Cs_2O}(100 - x)\mathrm{ZMW}(0 < x < 10)$, where

Table 1. Nominal base compositions of the borosilicate glass systems before addition of Cs_2O.

System	Mol% SiO_2	Mol% B_2O_3	Mol% Na_2O	Mol% Li_2O	Mol% Al_2O_3, La_2O_3, MgO	Mol% Fe_2O_3	R
MW	60.61	18.57	10.53	10.29	—	0.1	1.12
AlMW	60.03	18.39	10.43	10.19	0.95	0.1	1.07
LaMW	59.59	18.26	10.35	10.12	1.68	0.1	1.03
MgMW	59.06	18.10	10.26	10.03	2.55	0.1	1.26
Mg′MW	54.43	16.68	9.46	9.24	10.20	0.1	1.73

ZMW represents a variety of simulated base glasses to which caesium oxide is added (table 1). These four base glasses are modifications of the base-glass composition (MW) used by BNFL Ltd for high level nuclear waste (HLW) vitrification, with a further oxide added, in a quantity realistic of that in HLW. These additional oxides (and their initial molar quantities, y, before the addition of caesium oxide) are: Al_2O_3 (0.95 mol%), La_2O_3 (1.68 mol%) and MgO (2.55 and 10.20 mol%). The parent base glass MW is scaled down proportionally in the form $y[Al_2O_3, La_2O_3, MgO](100 - y)$MW to form the new base glasses, respectively, to which caesium oxide is added. The compositions of MW, and all the derived base glasses, prior to Cs_2O addition, are given in table 1.

For each system, 100 g batches were made with the appropriate combinations of reagent grade lithium carbonate (99.9%), sodium carbonate (99.95%), caesium carbonate (99.99%), aluminium oxide (99.9%), lanthanum oxide (99.99%), magnesium carbonate (99.9%), sodium tetraborate (99.5%) and Wacomsil© quartz (99.9%) with 0.1 mol% iron (III) oxide (99.5%) added to reduce NMR T_1 relaxation times. Samples were mixed on rollers for 24 h before being transferred to 90%Pt/10%Rh crucibles and heated to between 1350 and 1400 °C (depending on composition) for 20 min before being cast into de-ionized water to form a frit. Samples were then re-melted at the same temperature and cast. Samples were analysed using x-ray diffraction (XRD) to confirm their amorphous character.

2.2. Raman spectroscopy

Raman spectra were obtained at room temperature with a Renishaw Invia Raman spectrometer equipped with a 20 mW argon laser operating at 514 nm. Measurements reported here were acquired at room temperature with an incident laser power of 10 mW and a 50× objective. The spectrometer resolution was approximately 2 cm^{-1}.

2.3. ^{11}B MAS NMR

^{11}B MAS NMR spectra were obtained on a Varian/Chemagnetics Infinity 600 NMR spectrometer operating at 192.04 MHz with a Chemagnetics MAS 4 mm probe spinning at 15 kHz. For each sample, 1000 acquisitions were taken with a pulse delay of 1 s and a 0.7 μs pulse width ($B_1 \sim 60$ kHz). Samples were referenced against BPO_4 solid taken as −3.3 ppm with respect to the primary reference $Et_2O{:}BF_3$ at 0 ppm. Peak fits were made using the DMfit2002 NMR program [37].

2.4. ^{29}Si MAS NMR

^{29}Si MAS NMR was carried out using a CMX Infinity 360 NMR spectrometer operating at 71.25 MHz with a 6 mm probe spinning at 6 kHz. A 5 s pulse delay and 2 μs pulse width (30° tip angle) were used with ∼1000 acquisitions. Samples were referenced to tetramethylsilane (TMS) at 0 ppm. Peak fits were made using the DMfit2002 NMR program [37].

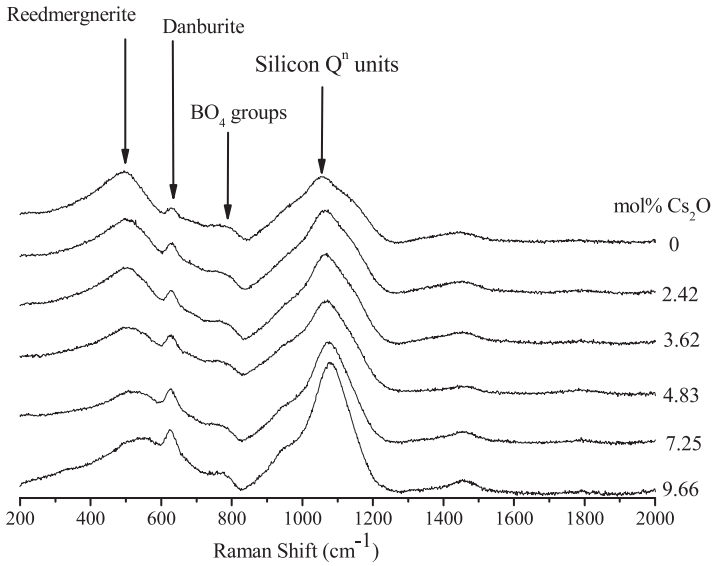

Figure 1. Typical Raman spectra for the CsAlMW system.

2.5. ^{27}Al MAS NMR

^{27}Al MAS NMR spectra were obtained on a Varian/Chemagnetics Infinity 600 NMR spectrometer operating at 156.03 MHz with a Chemagnetics MAS 4 mm probe spinning at 12 kHz. For each sample, 1000 acquisitions were taken with a pulse delay of 1 s and a 0.5 μs pulse width. Samples were referenced against YAG solid taken at 0 ppm.

3. Results

3.1. Sample preparation

The samples were amorphous within the limits of detection by XRD with no optical phase separation. This was expected, since R values (mol% alkali oxide/mol% boron oxide) for compositions in this study are outside the zone of immiscibility ($0.2 \leqslant R \leqslant 0.3$) where phase separation is found to occur [38].

3.2. Raman spectroscopy

Typical Raman spectra for the four systems are shown in figure 1. The background for each spectrum was subtracted by fitting an exponential curve to the uncorrected spectrum in a technique adapted from Mysen [39]. The region of the spectrum below approximately 200 cm^{-1} is truncated by equipment filters and so has been ignored in any analysis.

3.3. ^{11}B MAS NMR

The ^{11}B MAS NMR spectra show a large, relatively narrow peak from [BO_4] at ~0 ppm and a smaller, broader peak from [BO_3] at ~13 ppm, with figure 2(a) being representative of the ^{11}B MAS NMR spectra for all four systems. N_4 values were calculated from resolved peak areas obtained from the DMfit2002 NMR peak fitting program [37]. Spectra were fitted with four

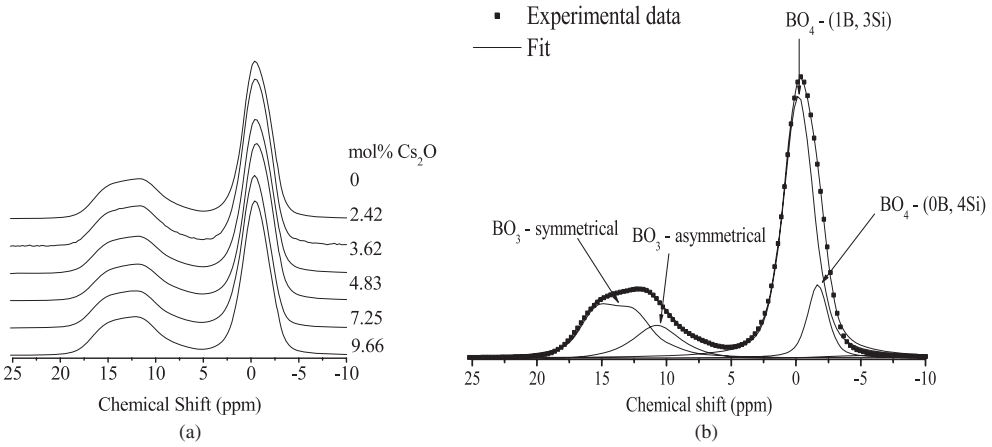

Figure 2. (a) Typical ^{11}B MAS NMR spectra for the CsLaMW system; (b) typical ^{11}B MAS NMR spectrum and fit.

peaks: two quadrupolar line-shapes, one for symmetric and one for asymmetric [BO_3] sites, and two Gaussian–Lorentzian line-shapes representing [BO_4] peaks (a good approximation where the quadrupole coupling constant is very small). Previous ^{11}B MAS NMR work on borosilicate glasses [40, 30] had been carried out by fitting a single Gaussian–Lorentzian line-shape to the [BO_4] region of the spectrum, until ^{11}B MQMAS NMR work by Du *et al* [27] demonstrated the presence of two peaks, separated by ∼1.8 ppm. They assigned these peaks to boron atoms in sites similar to those in the borosilicate mineral superstructures, reedmergnerite and danburite units, i.e. [$B(OSi)_4$] and [$B(OB)(OSi)_3$] respectively. In fitting the B_4 peak, the positions were initially fixed to mean values reported by Du and Stebbins [27] and the fitting procedure run to see if peaks of realistic half-widths were obtained. Fits were judged to be unrealistic if the resolved half-width for the smaller peak (at ~ -2 ppm) was greater than 2 ppm. After this check, the peak positions were allowed to vary. The danburite peak was found at ~ -0.2 ppm and the reedmergnerite peak at ~ -1.7 ppm, giving a separation of ∼1.5 ppm, and the widths are ∼2.7 and ∼2.0 ppm, respectively. The fraction of danburite-like units is obtained by dividing the fractional intensity by two to allow for the presence of twice as many B atoms in the danburite unit as the reedmergnerite unit. A typical fit is shown in figure 2(b).

N_4 values were corrected with the resolved [BO_3] fraction being increased by 4%. This increase is necessary due to the loss, under MAS, of central $(1/2, -1/2)$ transition intensity from the [BO_3] centre-band into the spinning side-bands. This does not happen for the $[BO_4]^-$ sites with their much smaller quadrupole interaction, so that all of the central $(1/2, -1/2)$ transition intensity appears in the centre-band [41].

3.4. ^{29}Si MAS NMR

A typical set of ^{29}Si MAS NMR spectra for the systems studied are shown in figure 3(a). The ^{29}Si MAS NMR spectra were fitted in most cases with two Gaussian lines: one Q^3 peak and one Q^4(B) peak, a silicon with one or more B next nearest neighbours (NNN). In the case of reedmergnerite, of the three Si in the unit, one Si has two B NNN and two Si have one B NNN. For danburite, both Si are identical, with three B NNN. Whilst these Si environments will each produce different chemical shifts, they are not resolvable in our spectra and therefore only one

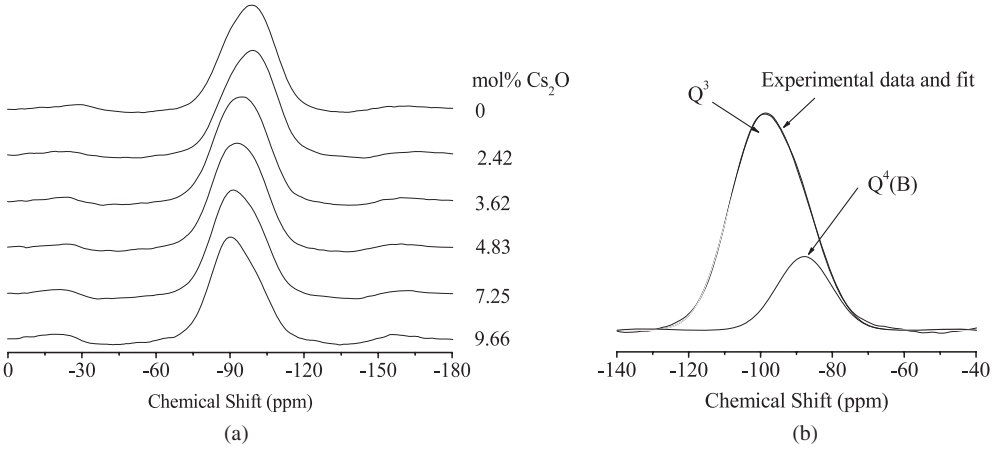

Figure 3. (a) Typical ^{29}Si MAS NMR spectra for the CsAlMW glass system; (b) typical ^{29}Si MAS NMR spectrum and fit.

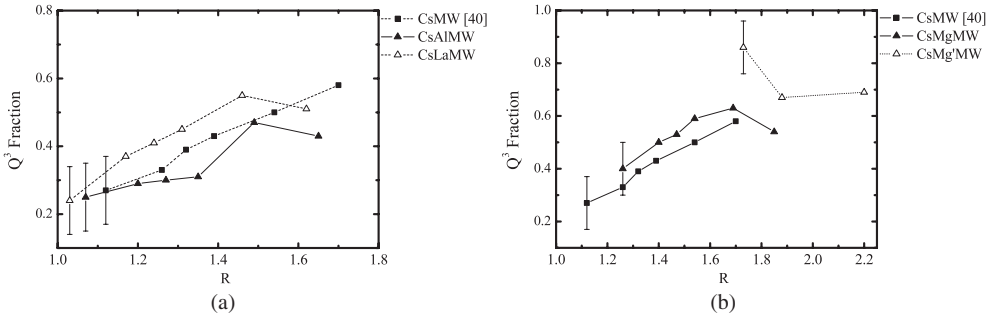

Figure 4. Resolved Q^3 fractions for (a) the CsAlMW and CsLaMW borosilicate systems; (b) the CsMgMW and CsMg′MW borosilicate systems. Values for the CsMW system are included for comparison [40].

Q^4(B) peak was used in the fitting procedure. Using the fraction of danburite determined from the ^{11}B spectra, the mean number of B NNN can be calculated as lying in the range 2–2.4. Contributions from Q^2 units were negligible for all but typically the highest Cs_2O content and the high MgO series, CsMg′MW. A typical fit is shown in figure 3(b). Resolved Q^3 fractions for all four systems were observed to increase nonlinearly (between 0.2 and 0.6) across the range of compositions (figures 4(a) and (b)).

3.5. ^{27}Al MAS NMR

The spectra are shown in figure 5, where it can be seen that the majority of Al are in four-coordinated sites, giving the resonance which peaks at ∼55 ppm. Some six-coordinated Al is also present. In the 0 mol% and 9.66 mol% Cs_2O samples, this gives a single sharp peak at ~ -2 ppm, superimposed on a broader peak (complicated by the spinning side-band) whereas, in the 2.42 and 4.83 mol% Cs_2O samples, there is a second sharp peak at ∼9.5 ppm which is of similar intensity. The total percentage of six-coordinated Al is ∼10%, with slightly more in the 4.83 mol% Cs_2O sample.

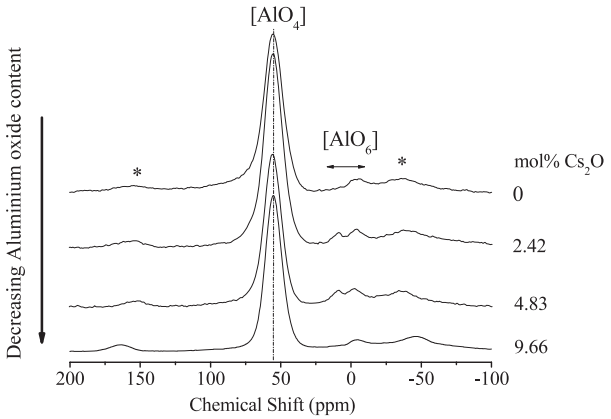

Figure 5. ^{27}Al MAS NMR spectra for the CsAlMW system.

4. Discussion

4.1. Raman spectroscopy

Peaks in the Raman spectra of all four systems have been identified by comparison with reports by Konijnendijk [36], Utegulov *et al* [25] and Bunker *et al* [26] on the Na_2O–B_2O_3–SiO_2, Al_2O–SiO_2–Na_2O–MgO–Eu_2O_3 and Na_2O–SiO_2–B_2O_3 glass systems, respectively. Peaks due to reedmergnerite (500 cm^{-1}) and danburite (634 cm^{-1}) units are observed (figure 1). Their presence explains the high N_4 values compared to binary borates [13, 42, 12], since the [BO_4] units are stabilized by adjacent [SiO_4] units.

4.2. ^{11}B MAS NMR

The changes in N_4 fraction with R, the ratio of total mol% alkali oxide to mol% boron oxide content for the CsAlMW and CsLaMW systems and for the CsMgMW and CsMg′MW systems, are shown in figures 6(a) and (b), respectively. In the systems containing intermediate oxides, R is calculated on the basis that every mole of intermediate present (i.e. Al_2O_3 and La_2O_3) removes one mole of alkali oxide to form $[ZO_n]^-M^+$ network units, where n is 4 for Al and 6 or 7 (including some bridging oxygens) for La. MgO is treated as a modifier for the purpose of calculating R, adding to the total molar contribution from the group I oxides present. N_4 values are compared in figure 6 with those obtained by Roderick [43], the Dell [14] model and our previous study on Cs_2O additions to MW [40]. For similar values of R, N_4 values for the four systems containing intermediate oxides are lower than both the prediction of the Dell model [14] and also the values observed for the systems composed of only group I (alkali) oxides CsMW [40, 43]. Therefore, the simple argument of the removal of alkali as a charge-compensating cation for the intermediate species is insufficient to explain the reduction in the fraction of four-coordinated borate units. A major consequence of the addition of these oxides is the promotion of the transfer of modifier alkali to the silicate network [44].

The danburite fraction, obtained from the two resolved peaks under the [BO_4] region of the ^{11}B MAS NMR spectrum (figure 7(a)), decreases from approximately 0.60 to 0.35 for the Al_2O_3 and La_2O_3 containing systems, and increases from 0.50 to 1.1 for the Group I alkali [40] and MgO-containing borosilicate systems (figure 7(b)). The presence of danburite-like units, with their B_4–O–B_4 connections, is surprising, given the usual tendency for charged units to

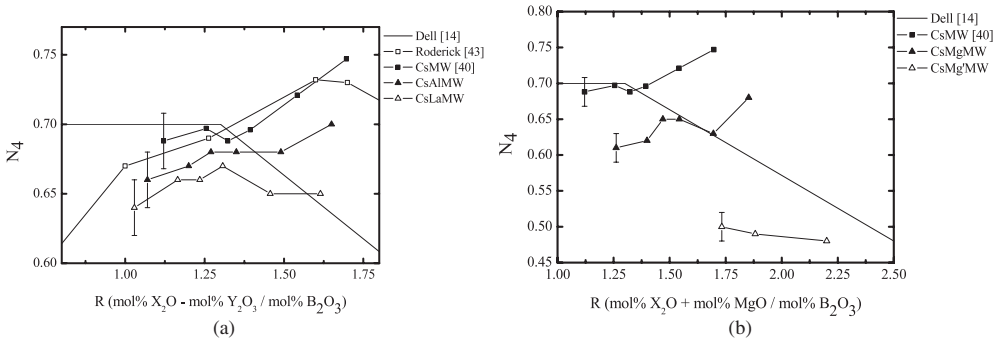

Figure 6. Resolved N_4 fractions for (a) the CsAlMW and CsLaMW borosilicate glass systems, and (b) the CsMgMW and CsMg′MW borosilicate glass systems, as a function of calculated R. Values for the CsMW system are included in each case for comparison [40]. The lines are the predicted values from the Dell model [14].

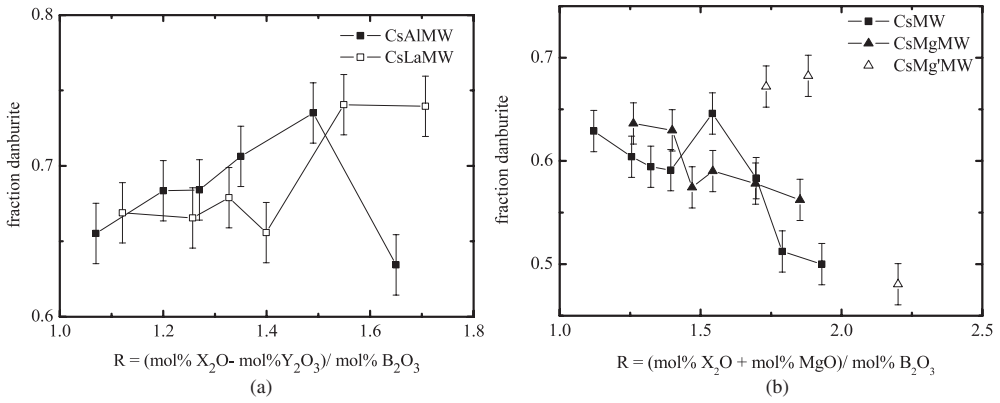

Figure 7. Ratio of resolved peaks under the [BO_4] region of the ^{11}B MAS NMR spectrum for (a) the CsAlMW and CsLaMW glass systems, and (b) the CsMgMW and CsMg′MW glass systems. Values for the CsMW system are included in the latter case for comparison. Note: the line is a guide to the eye.

avoid each other. Similar results have also been obtained by Du *et al* [38] in sodium borosilicate glasses with a range of K values, with the fraction of danburite units increasing (0–0.4) as a function of R ($0 \leqslant R \leqslant 0.7$).

On adding Cs_2O to the AlMW glass here, N_4 increases in parallel with the CsMW data (figure 6(a)), the displacement reflecting the modifier removed to charge compensate $[AlO_4]^-$. A similar situation arises for the La_2O_3 addition. In both of these cases, there is also an increase in the fraction of danburite units compared to reedmergnerite units. This is consistent with an increase in N_4, since danburite units contain twice as many B atoms compared to reedmergnerite units. The addition of MgO in small quantities produces a large reduction in N_4 initially, but the subsequent addition of Cs_2O again produces an increase in N_4 which parallels that of CsMW. However, in this case, the amount of danburite decreases relative to reedmergnerite.

4.3. ^{29}Si MAS NMR

Resolved Q^3 fractions, from ^{29}Si MAS NMR, for the four borosilicate systems (figures 4(a) and (b)) are larger than for the CsMW system [40] at equivalent values of R. This complements the ^{11}B MAS NMR results, which suggest that the introduction of Al_2O_3 and La_2O_3 into the Cs(MW) system not only reduces the amount of alkali modifier bonded to the borate network (lowering N_4) but also results in the transfer of alkali species to the silicate network, increasing the fraction of Q^3 units. This is also observed for the CsMgMW and CsMg′MW systems (figure 6), where Q^3 is also greater than originally observed in the CsMW system [40].

4.4. ^{27}Al MAS NMR

The position of the four-coordinated Al peak of ∼55 ppm is typical of $[Al(OSi)_4]$ rather than $[Al(OB)_4]$(∼40–45 ppm) and means that the Al_2O_3 addition is associating specifically with silicate polyhedra. It is possible that $[AlO_4]$ units substitute for $[BO_4]$ units in reedmergnerite or danburite. However, there is overwhelming evidence that $[AlO_4]^-$ units avoid each other in aluminosilicates. Therefore, we would not expect $[AlO_4]^-$ to substitute for $[BO_4]^-$ in the danburite units. Du and Stebbins [32] found that the mutual avoidance of $[AlO_4]$ and B_4 in aluminoborate glasses is less pronounced than for B_4–B_4 or $[AlO_4]$–$[AlO_4]$. In a subsequent study on aluminoborosilicate glasses [45], they observed that $[AlO_4]$–B_4 avoidance is a major factor where only monovalent cations are available for charge balancing. The origin of the six-coordinated Al units is not known. The sharper features may arise from a crystalline impurity phase(s)—possibly aluminosilicate in nature. Their overall abundance is too low for crystalline peaks to be detected by x-ray diffraction.

4.5. Structural implications

The ^{11}B NMR spectra have been used to calculate the relative amounts of the two MRO units, reedmergnerite and danburite, which have been identified by previous workers using Raman spectroscopy [25, 26] and NMR [27]. This information can be used, in conjunction with the fraction of Q^4 units obtained from ^{29}Si NMR, to calculate the proportion of Q^4 units which are not associated with these MRO units. If there are b moles of B_2O_3 and s moles of SiO_2 in glass, with N_4 (fraction of four-coordinated borons), f_D (the fraction of danburite) and Q^3 (the fraction of Q^3 units) measured experimentally, then the number of boron atoms in the danburite units, B_4D, is given by

$$B_4D = 4^*b^*N_4^*f_D/(1 + f_D), \tag{1.1}$$

and the number of boron atoms in the reedmergnerite units is given by

$$B_4R = B_4 - B_4D. \tag{1.2}$$

The boron next-nearest neighbours are four Si for reedmergnerite borons and one B + three Si for the danburite borons. Assuming that there is B_4/Q^3 avoidance, because of their charges, then the number of Si ($= Q^4$) connected to the boron atoms in the MRO units is given by

$$0.75^*B_4D + B_4R. \tag{1.3}$$

Some of these Q^4 will be members of the MRO units. The number of Q^4 not connected to MRO boron atoms (referred to as non-MRO Q^4) is then given by

$$s^*(1 - Q^3) - (0.75^*B_4D + B_4R). \tag{1.4}$$

(Note that this does not exclude Q^4 connected to ring silicon atoms.) The percentages of Q^4 units that are not connected to MRO boron atoms are compared with those in the MRO units

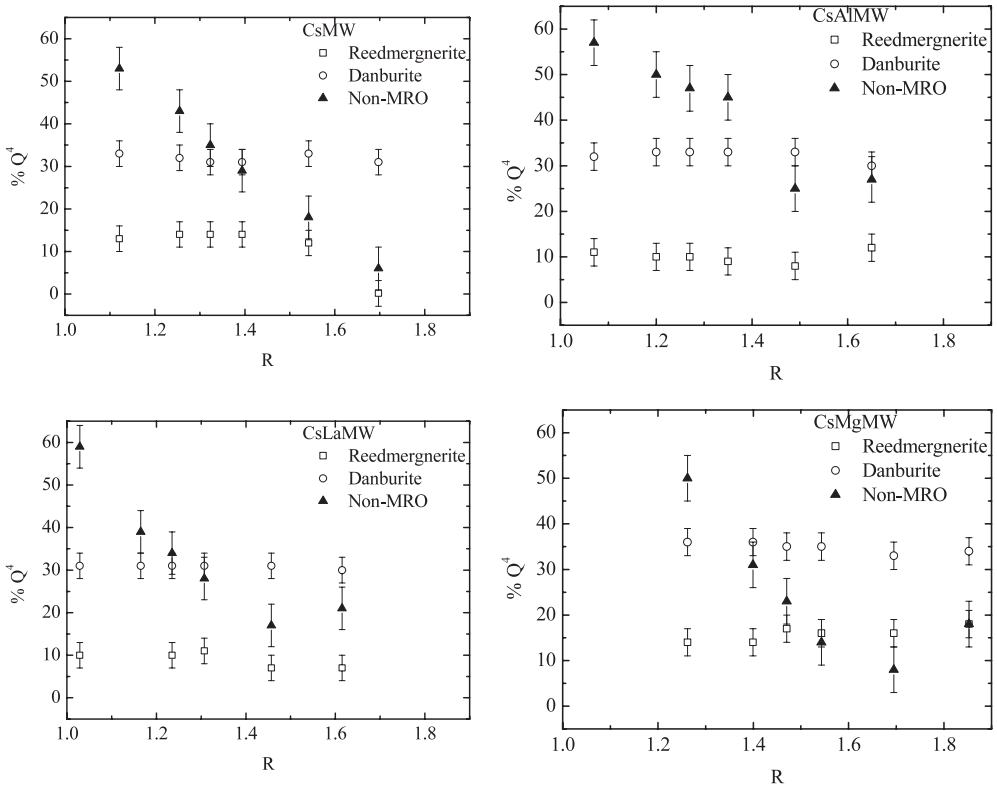

Figure 8. Resolved Q^4 fractions (reedmergnerite, danburite and non-MRO units) for CsMW, CsAlMW, CsLaMW and CsMgMW.

as a function of R for the various systems in figure 8. Figure 9 compares the amounts of non-MRO Q^4 for the various systems. The high MgO system, CsMg′MW, is not included in these calculations because of the large fraction of Q^2 units that are present in these samples. Figure 8 shows that the fractions of Q^4 units that are associated with the MRO units remain remarkably constant as R changes and it is the non-MRO Q^4 units which decrease, indicating that it is these which are preferentially converted to Q^3. Figure 9 shows that the rate of removal of the non-MRO Q^4 units is largely independent of the minor additions of Al_2O_3 and La_2O_3 compared to the basic system CsMW, the main difference being an initial offset. The upturn at the end of three of the curves reflects the production of Q^2 at these R values. The similarity of these curves is in contrast to the differences seen in the Q^3 versus R plots (figure 4) which reflect the corrosion and volatilization tendencies of these systems [38].

5. Conclusions

Boron-11 MAS NMR measurements on four mixed oxide–borosilicate glasses have shown that the fraction of four-coordinated boron units differs significantly from that predicted by earlier models, indicating that not only do intermediate network formers remove alkali groups from the borate network, but they also aid the transfer of alkali to silicate units. Superstructural units in the form of reedmergnerite and danburite have been detected with Raman spectroscopy, indicating that the borate and silicate networks are not separated and possibly account for the

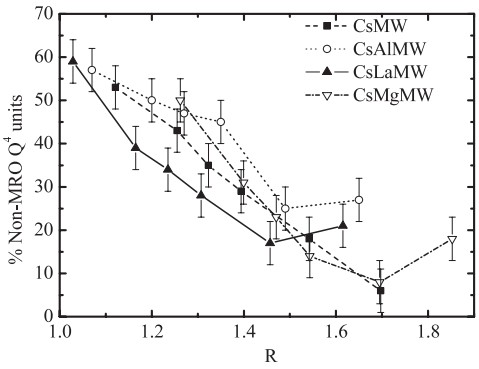

Figure 9. Comparison of the percentage of non-MRO units for CsMW, CsAlMW, CsLaMW and CsMgMW. (The lines are drawn to guide the eye.)

high (∼0.7) values of N_4. The presence of both of these medium-range order units in the Raman spectroscopy data gives confidence that there is more than one contribution to the [BO_4] peak in the ^{11}B MAS NMR spectra. The ratio of these two peaks (reedmergnerite/danburite) decreases as a function of caesium oxide content when intermediate oxides such as aluminium or lanthanum are present, and increases when either magnesium or group I alkali oxides alone (R: Li, Na, K, Cs) are present. The proportion of Q^4 units which are not connected to the boron atoms decreases with R in a similar fashion for all of the systems, and it is the concentration of Q^3 species which controls the thermal and chemical resistance of these materials.

Acknowledgments

The authors would like to thank British Nuclear Fuels Ltd for their financial support and the UK Engineering and Physical Science Research Council (EPSRC) and the University of Warwick for partial funding of the NMR facility.

References

[1] Zachariasen W H 1932 *J. Am. Chem. Soc.* **54** 3841
[2] Bureau B, Troles J, Le Floch M, Smektala F and Lucas J 2003 *J. Non-Cryst. Solids* **326/237** 58
[3] Cabaret D, Le Grand M, Ramos A, Flank A-M, Rossano S, Galoisy L, Calas G and Ghaleb D 2001 *J. Non-Cryst. Solids* **289** 1
[4] Chemarin C and Champagnon B 1999 *J. Non-Cryst. Solids* **243** 281
[5] Yiannopoulos Y D, Varsamis C P E and Kamitsos E I 2002 *Chem. Phys. Lett.* **359** 246
[6] Mamedov S, Bolotov A, Brinker L, Kisliuk A and Soltwisch M 1998 *J. Non-Cryst. Solids* **224** 89
[7] Santos L F and Almeida R M 1998 *J. Non-Cryst. Solids* **232–234** 638
[8] Gaskell P H 2005 *J. Non-Cryst. Solids* **351** 1003
[9] Anguiar P M and Kroeker S 2005 *Solid State Nucl. Magn. Reson.* **27** 10
[10] Bertmer M, Zuchner L, Chan C C and Eckert H 2000 *J. Phys. Chem.* B **104** 6541
[11] Borjesson L, Torell L M, Dahlborg U and Howells W S 1989 *Phys. Rev.* B **39** 3404
[12] Bray P J and O'Keffe J G 1963 *Phys. Chem. Glasses* **4** 37
[13] Clarida W J, Berryman J R, Affatigato M, Feller S A, Kroeker S, Ash J, Zwanziger J W, Meyer B M, Borsa F and Martin S W 2003 *Phys. Chem. Glasses* **44** 215
[14] Dell W J, Bray P J and Xiao S Z 1983 *J. Non-Cryst. Solids* **58** 1
[15] Kamitsos E I and Chryssikos G D 1991 *J. Mol. Struct.* **247** 1
[16] Kodama M, Nakashima N and Matsushita T 1993 *Japan. J. Appl. Phys.* **32** 2227
[17] Kroeker S and Stebbins J F 2001 *Inorg. Chem.* **40** 6239

[18] Meera B N and Ramakrishna J 1991 *J. Non-Cryst. Solids* **159** 1
[19] Zhong J and Bray P J 1989 *J. Non-Cryst. Solids* **111** 67
[20] Sinclair R N, Haworth R, Wright A C, Parkinson B G, Holland D, Taylor J W, Vedishcheva N M, Polyakova I G, Shakhmatkin B A, Feller S A, Rijal B and Edwards T 2006 *Phys. Chem. Glasses: Eur. J. Glass Sci. Technol.* B **47** 4
[21] Sinclair R N, Stone C E, Wright A C, Polyakova I G, Vedishcheva N M, Shakhmatkin B A, Feller S A, Johanson B C, Venhuizen P, Williams R B and Hannon A C 2000 *Phys. Chem. Glasses* **41** 286
[22] Veksler I V, Dorfman A M, Dingwell D B and Zotov N 2002 *Geochim. Cosmochim. Acta* **66** 2603
[23] Konijnendijk W L and Stevels J M 1975 *J. Non-Cryst. Solids* **18** 307
[24] Kroeker S, Feller S A, Affatigato M, O'Brien C P, Clarida W J and Kodama M 2003 *Phys. Chem. Glasses* **44** 54
[25] Utegulov Z N, Wickstead J P and Shen G-Q 2004 *Phys. Chem. Glasses* **45** 166
[26] Bunker B C, Tallant D R, Kirkpatrick R J and Turner G L 1990 *Phys. Chem. Glasses* **31** 30
[27] Du L-S and Stebbins J F 2003 *J. Non-Cryst. Solids* **315** 239
[28] Jellison G E, Feller S A and Bray P J 1978 *Phys. Chem. Glasses* **19** 52
[29] Feller S A, Dell W J and Bray P J 1982 *J. Non-Cryst. Solids* **51** 21
[30] Roderick J M, Holland D, Howes A P and Scales C R 2001 *J. Non-Cryst. Solids* **293–295** 746
[31] Chen D, Miyoshi H, Masui H, Akai T and Yazawa T 2004 *J. Non-Cryst. Solids* **345/346** 104
[32] Du L-S and Stebbins J F 2005 *Solid State Nucl. Magan. Reson.* **27** 37
[33] Luckscheiter B and Nesovic M 1996 *Waste Manage.* **16** 571
[34] Kim K S and Bray P J 1974 *Phys. Chem. Glasses* **15** 47
[35] Dwivedi B P, Rahman M H, Kumar Y and Khanna B N 1993 *J. Phys. Chem. Solids* **54** 621
[36] Konijnendijk W L and Stevels J M 1975 *J. Non-Cryst. Solids* **20** 193
[37] Massiot D, Fayon F, Capron M, King I, Le Calve S, Alonso B, Durand J O, Bujoli B, Gan Z and Hoatson G 2002 *Magn. Reson. Chem.* **340** 70
[38] Du L-S and Stebbins J F 2003 *J. Phys. Chem.* B **107** 10063
[39] Mysen B O 1990 *Am. Mineral.* **75** 120
[40] Parkinson B G, Holland D, Smith M E, Howes A P and Scales C R 2005 *J. Non-Cryst. Solids* **351** 2425
[41] Mackenzie K J D and Smith M E 2002 *Multinuclear Solid-State NMR Inorg. Mater.* **6** 424–31
[42] Berryman J R, Feller S A, Affatigato M, Kodama M, Meyer B M, Martin S W, Borsa F and Kroeker S 2001 *J. Non-Cryst. Solids* **293–295** 483
[43] Roderick J M 2001 A characterisation and radiation resistance study of a mixed-modifier borosilicate glass for HLW vitrification *PhD Thesis* Warwick University
[44] Park M J, Kim K S and Bray P J 1979 *Phys. Chem. Glasses* **20** 31
[45] Du L-S and Stebbins J F 2005 *J. Non-Cryst. Solids* **351** 3508